Molecular Crystals and Liquid Crystals

ISSN: 1542-1406 (Print) 1563-5287 (Online) Journal homepage: http://www.tandfonline.com/loi/gmcl20

Charge transfer modulated photochromic reactivity by incorporation picolylamine to a diarylethene unit

Xiaochuan Li, Guangqian Ji, Wooram Oh & Young-A Son

To cite this article: Xiaochuan Li, Guangqian Ji, Wooram Oh & Young-A Son (2016) Charge transfer modulated photochromic reactivity by incorporation picolylamine to a diarylethene unit, Molecular Crystals and Liquid Crystals, 636:1, 1-9, DOI: 10.1080/15421406.2016.1200929

To link to this article: http://dx.doi.org/10.1080/15421406.2016.1200929

Published online: 01 Nov 2016.

MOLECULAR CRYSTALS AND LIQUID CRYSTALS
2016, VOL. 636, 1–9
http://dx.doi.org/10.1080/15421406.2016.1200929

Taylor & Francis
Taylor & Francis Group

Charge transfer modulated photochromic reactivity by incorporation picolylamine to a diarylethene unit

Xiaochuan Li[a], Guangqian Ji[a], Wooram Oh[b], and Young-A Son[b]

[a]Collaborative Innovation Center of Henan Province for Green Manufacturing of Fine Chemicals, Key Laboratory of Green Chemical Media and Reactions, Ministry of Education, School of Chemistry and Chemical Engineering, Henan Normal University, Xinxiang, Henan, P. R. China; [b]BK21, Department of Advanced Organic Materials Engineering, Chungnam National University, South Korea

ABSTRACT

A photochromic triangle terthiophene with DPA attached compound was synthesized conveniently and fully characterized. The photochromic behavior was investigated before and after the addition of Zn^{2+} to the solution of **PT**. It was found that the PET effect, induced by DPA, suppressed the photochromic reactivity of **PT**. Upon the addition of Zn^{2+}, the photochromic reactivity was recovered and light pink color was observed under irradiation of 254 nm light. Different metal ions were also added and verify the single chelation towards Zn^{2+} with **PT**. Molecular geometric structures were optimized and HOMO/LUMOs were calculated with *DMol*^{3}. Two key factors, the distance of reactive carbon atoms and the LUMO distribution of **PT**-Zn favored it cyclization/cycloreversion triggered by photons.

KEYWORDS

photochromic; Zn^{2+}; PET; HOMO/LUMO; geometric structures

Introduction

Molecular switch is now one of the research focuses that has been developed intensively in the last decades and have been applied in molecular electronics, such as optical data storage, molecular assembling, logic system, and digital design [1–8]. The property that attractive chemists and physicists is the switch molecules that can be toggled between two well-defined states by external excitation (light, acid/base, ions, etc). Up to now, several photochromic systems have been well-established due to their excellent yields of photocyclization-photocycloreversion reactions, fatigue resistance, and thermal stability. Among variety of switch modes, diarylethene stood out of them with conveniently modified framework and tunable properties. Generally, the hexatriene framework of diarylethene could be cyclized driven by shorter wavelength light (UV) and the colorless state of diarylethene will transfer to the color state. Excited the color state of diarylethene with longer wavelength light (visible light), it will return to the original colorless state [9–11]. Thus, a molecular switch is established. The two well-defined states of diarylethene have distinct physical properties, such as conductance, emission intensity, viscosity, and refractive index. Reversible control of the corresponding physical parameters in the switching process can be utilized in signal translation and thus realized logic operation and mass-calculation in molecular level.

CONTACT Xiaochuan Li lixiaochuan@htu.cn School of Chemistry and Chemical Engineering, Henan Normal University, East Jianshe Rd. 46, Xinxiang, Henan, 453007, China; Young-A Son yason@cnu.ac.kr Department of Advanced Organic Materials Engineering, Chungnam National University, 220 Gung-dong, Daejeon, 305-764, South Korea.
Color versions of one or more of the figures in the article can be found online at www.tandfonline.com/gmcl.

In this contribution, triangle terthiophene (**TT**), a photochromic unit, was configured. And only one α position was left, which can be easily captured by strong base and transferred to aldehyde by treating with DMF. Next, required functional group could be attached to the α-position of **TT**. Here, di-(2-picolyl)amine (DPA), as an well-known metal ions chelating unit, was attached to the photochromic **TT** [12–14]. Our intension was to investigate the effect of photo-induced electron transfer (PET) and its response to metal ions, especially Zn^{2+}.

Experimental

General procedures and materials

The solvents used in the reaction were carefully dried according to the standard procedure and stored over 4Å molecular sieve. All the reagent-grade chemicals were purchased from Sigma-Aldrich CO. LLC. (South Korea) and used without further purification. Melting points were determined on a Mel-Temp® IA9200 digital melting point apparatus in a glass capillary and were uncorrected. All synthesized compounds were routinely characterized by TLC and ^{1}H NMR. TLC was performed on aluminum-backed silica gel plates (Merck DC. Alufolien Kieselgel 60 F254).

^{1}H and ^{13}C NMR spectroscopy

^{1}H and ^{13}C nuclear magnetic resonance (NMR) spectra were recorded on a Brucker AM-400 spectrometer operating at frequencies of 400 MHz for proton 100 MHz for carbon in $CDCl_3$. Proton chemical shifts (δ) are relative to tetramethylsilane (TMS, $\delta = 0$) as internal standard and expressed in parts per million. Spin multiplicities are given as *s* (singlet), *d* (doublet), *t* (triplet), and *m* (multiplet) as well as *b* (broad). Coupling constants (*J*) are given in Hertz.

High resolution mass spectra (HRMS)

The mass spectra measured on a LC-MS (Waters UPLC-TQD) mass spectrometer. High resolution mass spectra (HRMS) were measured on a Brucker micrOTOF II Focus instrument.

UV-Vis and emission spectra

The absorption spectra were measured with a PERSEE TU-1900 and an Agilent 8453 spectrophotometer. Emission spectra were measured with Shimadzu RF-5301PC fluorescence spectrophotometer. The solvents used in photochemical measurement were spectroscopic grade and were purified by distillation. The stock solution of compounds (2×10^{-3} M) was prepared in CH_3CN, and a fixed amount of these concentrated solutions were added to each experimental solution. All the experiments were done repeatedly, and reproducible results were obtained. Prior to the spectroscopic measurements, solutions were deoxygenated by bubbling nitrogen through them.

Theoretical calculations

For the theoretical study of the excited state photo-physics of the dye, the *DMol*^{3} program, which is available as part of *Material Studio* (Accelrys Inc., San Diego, California, United States), was used. Both the ground state geometries and the frontier molecular orbital of the

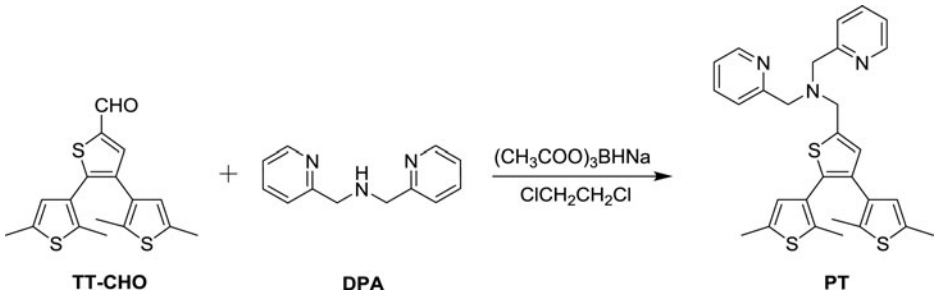

Scheme 1. Synthesis of **PT**.

dye were calculated using the density function theory (DFT) with the B3LYP hybrid functional and the double numerical plus *d*-functions (DND) atomic orbital basis set.

Synthesis

Synthetic routes of the target compound, 5-*N,N*-bis(pyridin-2-ylmethyl)methanamine-TT (**PT**), are outlined in Scheme 1. Firstly, the hydrogen atom at α position of TT was lithiation under lower temperature and then aldehyde was introduced by treating with anhydrous DMF [15]. Subsequently, reductive amination reaction was carried out between TT-CHO and DPA in the presence of sodium triacetoxyborohydride, which produced **PT**.

*5-N,N-bis(pyridin-2-ylmethyl)methanamine-TT (**PT**)*

TT-CHO (66 mg, 0.2 mmol) and sodium triacetoxyborohydride (855 mg, 0.4 mmol) were dissolved in dichloroethane (20 mL) and stirred at room temperature for 0.5h. Then di-(2-picolyl)amine (DPA) (48 mg, 0.24 mmol) was added to the mixture. The mixture was stirred for 8h continually in the dark. After the starting materials were full reacted, as confirmed by TLC, the mixture was poured into water (30 mL). Next, it was extracted with chloromethane (3×20 mL). The organic phase was combined and dried over anhydrous $MgSO_4$. After the solvent was evaporated in vacuum, the residue was loaded to the column. Column separation (silica gel 200-300 mesh, eluent: dichloromethane/methanol = 100/3) produced 40 mg viscous liquid (40%).

^{1}H NMR(400 MHz, $CDCl_3$): δ (ppm): 8.54 (2H, *d*, $J = 8.0$ Hz), 7.72 (4H, *d*, $J = 4.0$ Hz), 7.20 (2H, *q*, $J = 4.0$ Hz), 6.93 (1H, *s*), 6.49 (1H, *s*), 6.38 (1H, *s*), 4.02 (4H, *s*), 3.98 (2H, *s*), 2.37 (3H, *s*), 2.35 (3H, *s*), 2.00 (3H, *s*), 1.97 (3H, *s*). ^{13}C NMR (100 MHz, $CDCl_3$): δ (ppm): 148.3, 137.6, 135.4, 135.2, 134.1, 133.9, 133.2, 132.7, 130.6, 129.7, 127.5, 127.1, 123.7, 122.7, 58.8, 53.3, 15.1, 13.9, 13.8. HRMS (ESI): $[M+H]^+$ $C_{29}H_{30}N_3S_3$ requires 516.1602; found $[M+H]^+$ 516.1599.

Result and discussion

The photochromic behavior of **PT** was investigated in CH_3CN under irradiation of light and shown in Fig. 1. It can be seen that the maximum absorption band is positioned around 250 nm, which is matched to the wavelength of our daily used UV lamp in the lab. Upon irradiation of 254 nm UV light, no observable color state was observed. Only a very slightly absorption increase exhibited around 350 nm due to a π-π^* transition. Correspondingly, a gradually absorption decrease exhibited around 250 nm. Generally, the absorption band of ring-open form was positioned at shorter wavelength. The absorption peak extended to

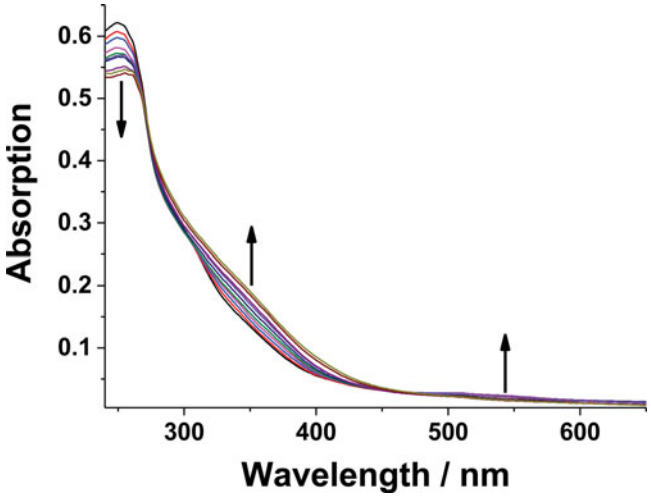

Figure 1. Absorption changes of **PT** in CH_3CN solution (1.0×10^{-5} M) upon irradiation with 254 nm light every 5 s.

longer wavelength for the ring-closed form due to the delocalization of π-electrons to cyclizing thiophene rings. The absorption increase of **PT** in the visible region (~550 nm) is nearly unobservable, indicating a very weak photo-cyclization reaction with 254 nm excitation. A well-defined isobestic point appeared at 273 nm ($\varepsilon = 7.1\times 10^4$ M^{-1} cm^{-1}), supporting the two component photochromic reaction. Reversibly, the 350 nm absorption band increased by irradiation with 365 nm and could be recovered to the original state.

Upon addition of equivalent of Zn^{2+}, the photochromic behavior of **PT** was enhanced. With similar approaches, the solution of **PT**-Zn was irradiated with 254 nm UV light and the absorption profile was shown in Fig. 2. The absorption profile was similar to that of **PT** without irradiation of 254 nm light and the maximum absorption band was also found around 250 nm. Upon irradiation the CH_3CN solution of **PT**-Zn with UV light ($\lambda = 254$ nm), a new absorption band centered at 538 nm emerged gradually with the formation of ring-closed

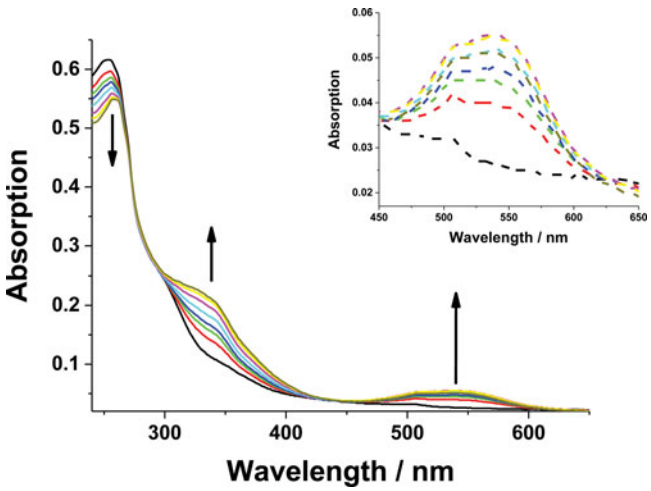

Figure 2. Absorption changes of **PT** in the presence of Zn^{2+} (1 equiv.) in CH_3CN solution (1.0×10^{-5} M) upon irradiation with 254 nm light every 5 s

from. Accompany with the absorption increasing of 350 and 538 nm, the absorption around 250 nm was decreased gradually. The newly emerged absorption band was positioned at visible region and this resulted to a light pink color of the solution. After 40 s irradiation, the absorption of **PT**-Zn reached to a photo-stationary state ($\varepsilon_{538nm} = 5.6\times 10^3\ M^{-1}\ cm^{-1}$). There was also an isobestic point formed at 273 nm. For the reverse reaction, the light pink solution of **PT**-Zn faded to colorless upon irradiation of visible light ($\geq$ 400 nm, LED lamp) and the absorption band centered at 538 nm disappeared gradually, producing an absorption spectrum identical to that of the initial solution of **PT**-Zn. The conversion efficiency (α_{ps}) between ring-open and ring-closed forms at the photo-stationary state, achieved by 254 nm light irradiation, was estimated to be 0.27, which was calculated following the expressions based on the absorbance of the two forms [16].

The activity of photochromism was suppressed significantly for **PT**. It can be considered to be the contribution of strong electron donation of DPA. Especially, the PET effect enhanced the electron density of photochromic core (**TT**). Particularly, the higher electron density of central thiophene ring of **TT** does not benefit to the photocyclization [17]. Once the Zn^{2+} was captured by DPA unit, the electron donor ability of N atom was decreased significantly. The photochromic activity was recovered, but not totally. If EDTA added to the solution of **PT**-Zn, the photochromic activity was suppressed again. The inactive-active cycling of photochromism was depicted in Scheme 2.

To illustrate the selectivity of Zn^{2+}, various different metal ions were also added to the solution of **PT** to verify its selectivity. After each of different metal ions was added, the solution of **PT** was irradiated with 254 nm UV light until the photo-stationary state reached. Fig. 3 shows the absorption of **PT** at 538 nm in photo-stationary state. It indicates that no distinct absorption change was observed in visible region induced by other metal ions, and established the selectivity of **PT** towards Zn^{2+}. Fatigue resistance is one of the key factors for reversible photoswitches, which requires the side reactions or decomposition of the corresponding compound as little as possible in each cyclization/cycloreversion cycle. 10 switch cycles was applied to **PT** and **PT**-Zn and photo-stationary state was reached each time with 254 nm excitation and then bleached to colorless with visible light (Fig. 4). Upon 4 switch cycles, there was about 20% and 10% degradation for **PT** and **PT**-Zn, respectively. 10 switch cycles later, the degradation of **PT** and **PT**-Zn reached to 56% and 30%, respectively. It is attested that **PT**-Zn is robust against photochemical decomposition than that of **PT**.

To better comprehend the geometrical, electronic, and optical properties of **PT** and **PT**-Zn, we undertook a comprehensive computational investigation using Material Studio. To reduce the run times in the first instance, the ground-state energy-minimized structures were calculated using DFT and LDA/DN basis set [18, 19]. Further refinement and optimization on structures were undertaken using DND/B3LYP basis set. Fig. 5 shows the optimized structure of **PT** and **PT**-Zn in antiparallel conformations. The ring-open forms of diarylethenes have two conformations, antiparallel and parallel, and the tow conformations interconvert with each other in solution. It is obvious that most of the molecules will adopt the conformations with lower molecular energy. Among numerous antiparallel and parallel conformations, there will be two representative antiparallel and parallel conformations with lowest energy state, respectively. As is known to all, only the antiparallel conformation could precede the conrotatory cyclization reaction under the irradiation of light. Additionally, the photocyclization reactivity of diarylethene is distance dependent rather than the polar and steric substituent effects, which has been well documented [20–22]. The distance between reactive carbon atoms of geometry optimized antiparallel conformations of **PT** and **PT**-Zn could be estimated to be 3.705 and 3.642 Å, respectively. Both of the two distances are shorter than 4.2 Å, the maximum

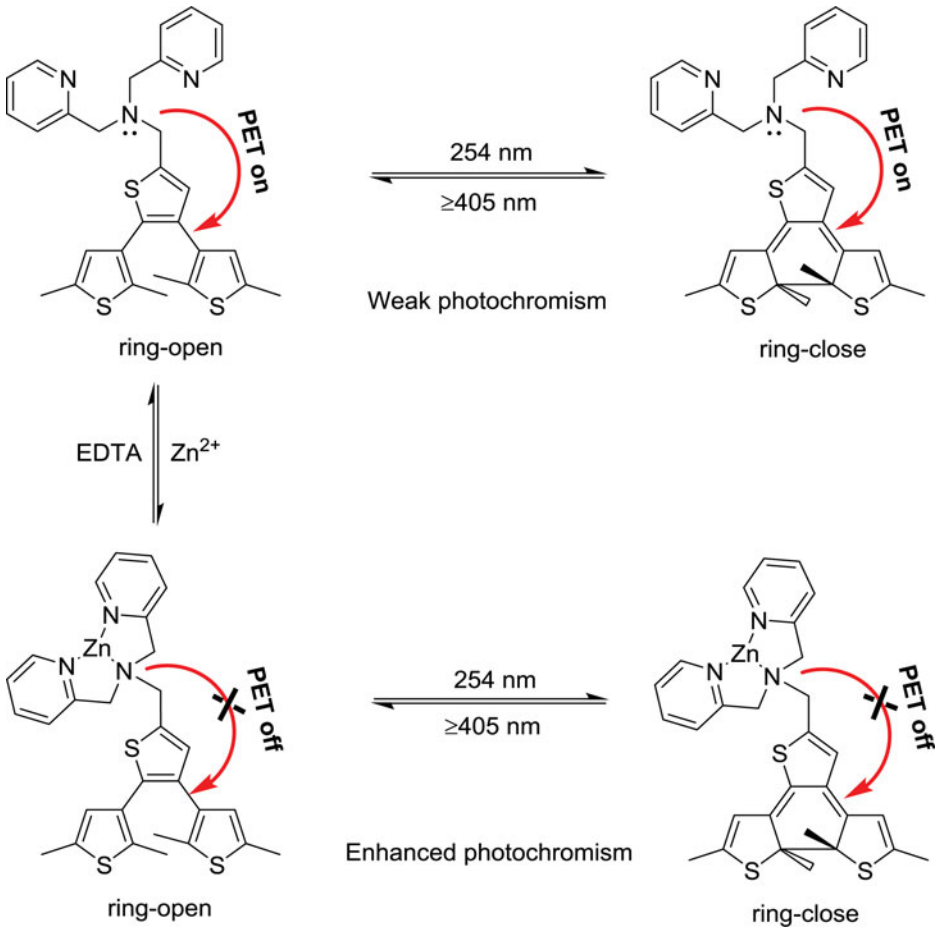

Scheme 2. Active and inactive cycle of photochromism of **PT** and **PT**-Zn

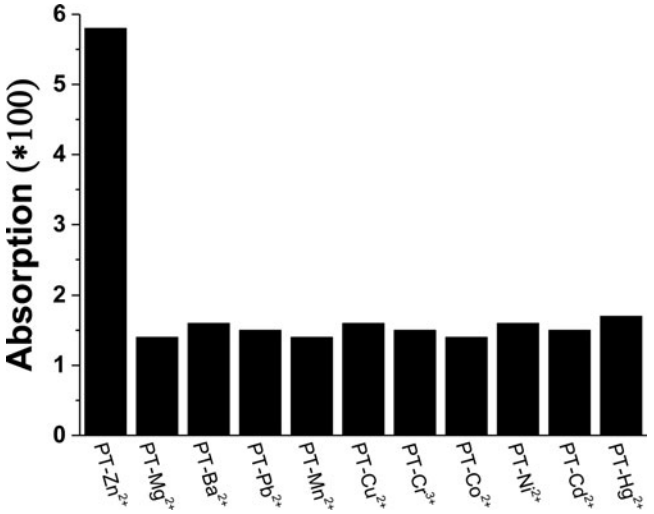

Figure 3. Absorption (538 nm) of **PT** with various metal ions addition (1 equiv.). Each time, the photostationary state was reached.

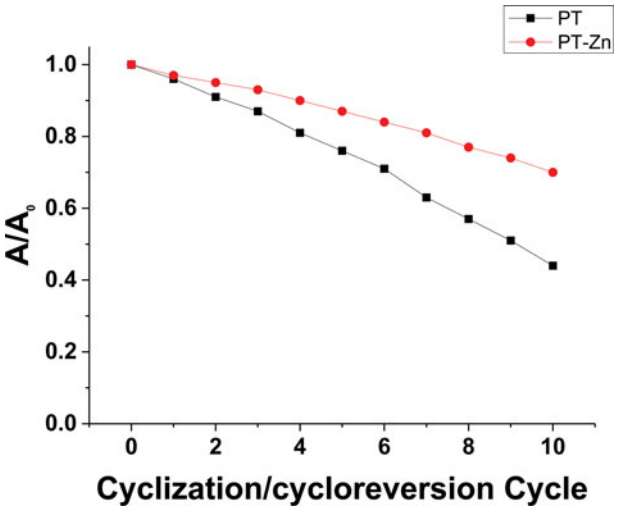

Figure 4. Fatigue resistance of **PT** and **PT**-Zn in CH_3CN. The wavelength was monitored at 273 nm.

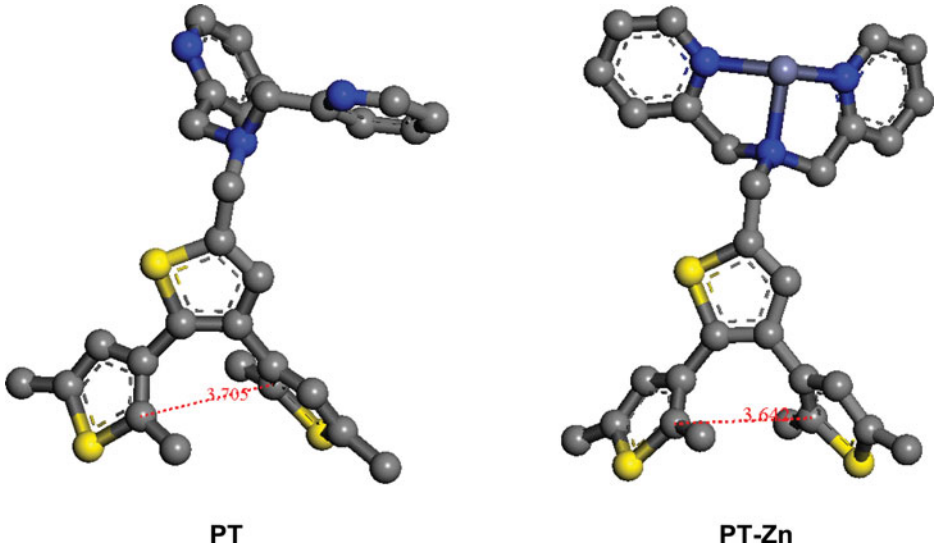

Figure 5. Optimized structure of **PT** and **PT**-Zn and the distance between reactive carbon atoms.

limit for photochromic activity. Once the distance between reactive carbon atoms exceeds the maximum limit, the photochromism will be totally suppressed. In case of **PT**-Zn, the distance is shorter than that of **PT**. It indicates that the photocyclization of **PT**-Zn could be more smoothly than that of **PT**.

The frontier molecular orbitals of **PT** and **PT**-Zn were also investigated with Time-Dependent Density Functional Theory (TD-DFT) based on the optimized ground state. Both of **PT** and **PT**-Zn exhibits absorption around 340 nm in longer wavelength, which corresponds to the quantum calculated value of 344 and 351 nm for **PT** and **PT**-Zn, respectively. The two π-$\pi*$ are dominated by HOMO-LUMO transition with the oscillator strengths (*f*) larger than 0.3. The topologies of molecular orbitals of **PT** and **PT**-Zn are shown in Fig. 6 and both have π shapes. The HOMO distributions of **PT** and **PT**-Zn have similar character with most of the electron density spread over the photochromic core. Only small part of

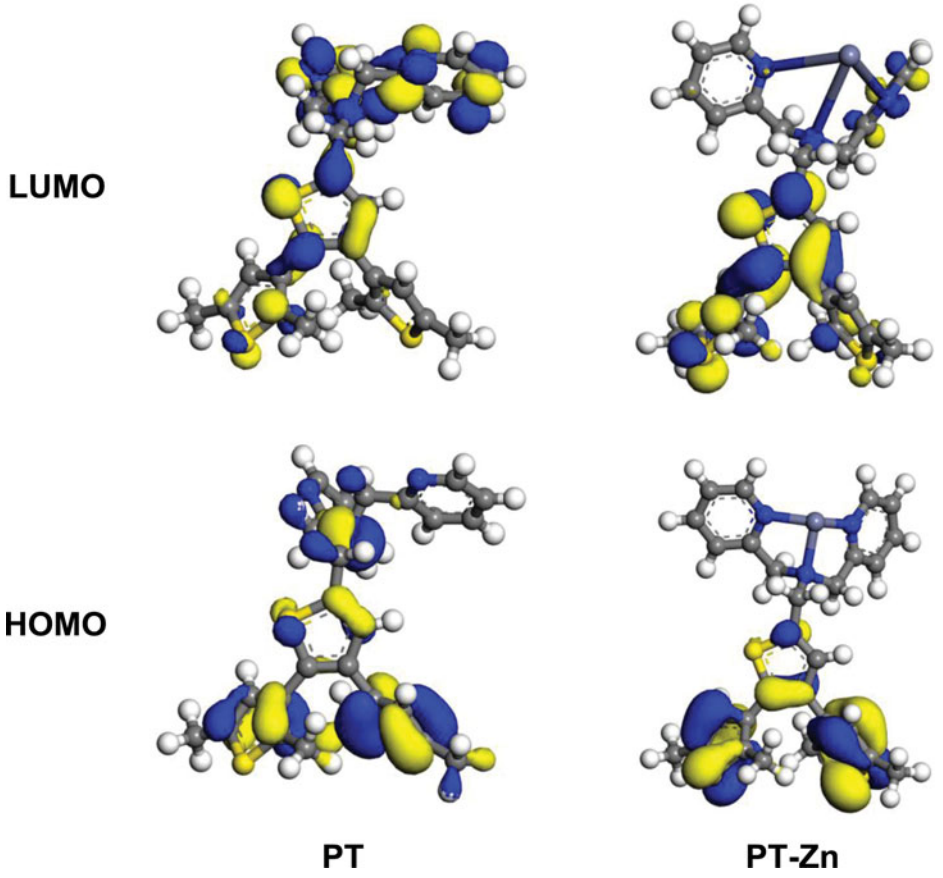

Figure 6. Frontier orbitals for **PT** and **PT**-Zn.

electron density delocalized toward DPA unit for the HOMO of **PT**. However, their LUMO distribution is distinctly different. For **PT**, the LUMO distribution is mainly positioned in DPA unit and only small part of electron density spread to one of photocyclizaton carbon atom. For **PT**-Zn, the electron distribution focused totally on the photochromic core, which is important for photochromism. To allow the ring-closing cyclization, the electron should be promoted into a state dominated by photochromic orbitals, which are characterized by a bonding nature for the to-be-formed carbon-carbon bond as well as a significant density on two or at least one reactive carbon atoms. Therefore, the LUMO distribution benefits to the photochromic activity of **PT**-Zn more than that of **PT**.

Conclusions

In summary, a photochromic derivative was configured with DPA attached and was full characterized. The photochromic behavior of **PT** and its Zn-chelate (**PT**-Zn) were investigated in detail in CH_3CN. Due to the intramolecular PET effect, the photochromism of **PT** was suppressed to a great extent. With Zn^{2+} addition to the solution of **PT**, the photochromism was recovered. Upon irradiation of 254 nm light, light pink color was observed with the emerging of 538 nm absorption. Various metal ions were also added and verify the singleness of Zn^{2+} induced intramolecular PET off. Based on the optimized structures of **PT** and **PT**-Zn, the distance between reactive carbon atoms were shorter than the threshold of 4.2 Å, which is

critical to the photochromic reactivity. The shorter reactive carbon atom distance of **PT**-Zn led to its higher photochromic reactivity than that of **PT**. The calculated molecular orbitals indicate that the electron location of **PT**-Zn delocalized to reactive carbon atoms in LUMO and is benefit to induce photocyclization reaction. The controllable photochromic activity can be used in configuration of molecular logic system and application of smart materials. Our work along those lines is in progress.

Acknowledgments

This work was supported by the National Natural Science Foundation of China (21072048), PCSIRT (grant no. IRT1061), and the Program for Innovative Research Team in University of Henan Province (15IRTSTHN003). This study was supported by the National Research Foundation of Korea (NRF) funded by the Ministry of Science, ICT and Future Planning (Grant no. 2015063131).

References

[1] Uchida, K., Yamanoi, Y., Yonezawa, T., & Nishihara, H. (2011). *J. Am. Chem. Soc. 133*, 9329.
[2] Snegir, S. V., Marchenko, A. A., Yu, P., Maurel, F., Kapitanchuk, O. L., Mazerat, S., Lepeltier, M., Léaustic, A., & Lacaze, E. (2011). *J. Phys. Chem. Lett.*, *2*, 2433.
[3] Cao, X., Zhou, J., Zou, Y., Zhang, M., Yu, X., Zhang, S., Yi, T., & Huang, C. (2011). *Langmuir*, *27*, 5090.
[4] Zheng, H., Zhou, W., Yuan, M., Yin, X., Zuo, Z., Ouyang, C., Liu, H., Li, Y., & Zhu, D. (2009). *Tetrahedron Lett.*, *50*, 1588.
[5] Tsujioka, T., & Kondo, H. (2003). *Appl. Phys. Lett.*, *83*, 937.
[6] Tian, H., & Yang, S. (2004). *Chem. Soc. Rev.*, *33*, 85.
[7] Yao, X., Li, T., Wang, S., Ma, X., & Tian, H. (2014). *Chem. Commun.*, *50*, 7166.
[8] Tian, H. (2010). *Angew. Chem. Int. Ed.*, *49*, 4710.
[9] Li, X., Ma, Y., Wang, B., & Li, G. (2008). *Org. Lett.*, *10*, 3639.
[10] Li, X., & Tian, H. (2005). *Tetrahedron Lett.*, *46*, 5409.
[11] Li, X., Jiang, W., & Son, Y. (2014). *Mol. Cryst. Liq. Cryst.*, *602*, 1.
[12] Hafuka, A., Kando, R., Ohya, K., Yamada, K., Okabe, S., & Satoh, H. (2015). *Bull. Chem. Soc. Jpn.*, *88*, 939.
[13] Peng, X., Du, J., Fan, J., Wang, J., Wu, Y., Zhao, J., Sun, S., & Xu, T. (2007). *J. Am. Chem. Soc.*, *129*, 1500.
[14] Betancourt-Mendiola, M. L., Pena-Cabrera, E., Gil, S., Chulvi, K., Ochando, L. E., & Costero, A. M. (2014). *Tetrahedron*, *70*, 3735.
[15] Wong, H. -L., Tao, C. H., Zhu, N., & Yam, V. W. -W. (2011). *Inorg. Chem.*, *50*, 471.
[16] Giordano, L., Jovin, T. M., Irie, M., & Jares-Erijman, E. (2002). *J. Am. Chem. Soc.*, *124*, 7481.
[17] Liu, G., Pu, S., & Wang, R. (2013). *Org. Lett.*, *15*, 980.
[18] Delley, B. (1990). *J. Chem. Phys.*, *92*, 508.
[19] Delley, B. (2000). *J. Chem. Phys.*, *113*, 7756.
[20] Kobatake, S., Uchida, K., Tsuchida, E., & Irie, M. (2002). *Chem. Commun.*, *23*, 2804.
[21] Shibata, K., Muto, K., Kobatake, S., & Irie, M. (2002). *J. Phys. Chem. A*, *106*, 209.
[22] Kobatake, S., Irie, M., & Bull. (2004). *Chem. Soc. Jpn.*, *77*, 195.